POLITECNICO
MILANO 1863

SCUOLA DI INGEGNERIA INDUSTRIALE
E DELL'INFORMAZIONE

Executive Summary of the Thesis

Mathematical and numerical coupled models for aortic hemodynamics and cardiac perfusion

Laurea Magistrale in Mathematical Engineering - Ingegneria Matematica

Author: Luca Crugnola

Advisor: Prof. Christian Vergara

Co-advisor: Marco Fedele

Academic year: 2021-2022

1. Introduction

Each muscle of the human body needs an oxygen supply in order to function properly and the cardiac muscle, or *myocardium*, makes no exception. The oxygenated blood reaching the cardiac muscular tissue is called *myocardial perfusion* and is provided by a very specialized vascular structure, the *coronary circulation*. Thanks to the particular morphology of this circulation, we can divide its arteries into two groups: epicardial arteries (laying on the epicardial surface of the heart) and intramural vessels (penetrating inside the myocardium). Distinct epicardial coronary arteries supply different myocardial territories [1], so that the myocardium can be partitioned into *perfusion regions*, each of them supplied by a different artery.

The recent growth in computing power has allowed computational models to represent a non-invasive, practical and flexible approach to study cardiac perfusion both in physiological and pathological conditions. However, myocardial perfusion is a complex phenomenon involving different physical processes related to the cardiac function, such as blood dynamics inside large vessels and microvasculature, myocardial contraction, or electrical signal propagation. Indeed, coronary blood flow (CBF) is influenced by the contraction of the myocardium that shrinks the intramural vessels, increasing their resistance to flow during systole (such effect is more significant in the left heart due to the higher absolute pressure values). Therefore, a mathematical and numerical model able to provide a comprehensive description of this process is yet to be achieved. In particular, authors have mainly focused on the modeling of single physics or a coupling of few of them, often resorting to complexity reduction approaches (such as reduced order models), which rely on simplifying assumptions in order to investigate only certain features of blood dynamics. Although being well suited for particular applications, such complexity reduction approaches present some limitations that do not allow a complete description of the perfusion process, particularly in pathological cases. Thus, 3D complete models should be considered in these cases.

Regarding the epicardial coronary arteries, a common choice for a complete description of blood dynamics is to use the 3D formulation of the Navier-Stokes (NS) equations. On the other hand, an explicit description of the intramural vessels is unfeasible due to the computational

cost of performing numerical simulations in such a dense network of vessels, therefore porous media modeling approaches, which involve an homogenization of the myocardium, are often considered. In particular, authors have mostly decided to provide a complete 3D description of either the epicardial coronary arteries or the intramural vessels. An exception is represented by the computational model for myocardial perfusion proposed by Di Gregorio et al. in [2], which provides a complete 3D blood dynamics description from epicardial coronary arteries to the cardiac tissue. The same model was calibrated and validated in [3] using patient-specific clinical data.

The aim of this work is to increase the upstream capabilities of the model proposed in [2] by including the aortic root inside the computational domain. Therefore, the project moves in the direction of providing a more comprehensive description of the myocardial perfusion process. In particular, the new modeling framework couples a 3D Navier-Stokes problem inside aortic root and epicardial coronary arteries with a multi-compartment Darcy modeling of the myocardium, treated as a porous medium.

To this purpose, this project comprises several operative steps:

1. reconstruction of anatomical geometries of patient-specific aortic roots and generation of computational meshes on aortic root and epicardial coronary arteries;
2. introduction of a computational model for hemodynamics in aortic root and epicardial coronary arteries, selecting suitable boundary conditions and implementing the numerical methods needed to perform simulations;
3. computational fluid dynamics (CFD) simulations inside patient-specific aortic root and epicardial coronary arteries;
4. coupling of the hemodynamics model reported at point 2. with a multi-compartment Darcy model for the myocardium, thus including the aorta in the model proposed in [2];
5. application of the coupled model, including the aorta, to patient-specific geometries;
6. investigation of the reliability of the coupled model in reproducing patient-specific myocardial blood flow (MBF) maps.

2. Generation of computational domains

In this section we give a brief overview of the process going from clinical images to patient-specific computational domains. The starting point of the process are Coronary Computed Tomography Angiography (cCTA) images of four healthy patients (P1, P2, P3, P4) provided to us by Monzino Cardiology Centre, in Milan.

The same cCTA images were used in [3] in order to reconstruct anatomical geometries of the epicardial coronary arteries and the myocardium. Notice that, due to the contrast of the images, they managed to reconstruct only the left ventricle, thus in this work we considered the myocardial perfusion process only for this heart's chamber. This approach makes sense because an ischemic region located in the left ventricle can have a significant impact on the correct functioning of the heart, since this chamber regulates the whole systemic circulation.

Regarding anatomical geometries reconstruction, the new contribution of this work is the segmentation of patient-specific geometries of the aortic root, which was performed from the cCTA images using the free open-source software VMTK. In particular, a level set segmentation is applied after a Fast Marching or Colliding Fronts initialization combined with a Thresholding technique. The output of the geometry reconstruction process is a surface representing the internal boundary of the aortic wall, depicted in Figure 1 for patient P1 as an example.

Figure 1: Reconstructed anatomical geometry of the aortic root for patient P1.

Reconstructed aortic roots had to be connected with epicardial coronary arteries, available from [3], in order to generate the computational meshes where the 3D NS problem is numerically solved. The software VMTK and Paraview were

extensively used for these procedures, together with novel techniques developed in [4].
Due to the different characteristic lengths inside aortic root and epicardial coronary arteries, a spatially dependent mesh size was set, allowing an accurate description of the geometrical details of small arteries while guaranteeing an affordable computational cost of running numerical simulations in such meshes. To this purpose, each reconstructed aortic root is divided in three areas: aortic sinus, coronary roots and ascending aorta. In this project we are particularly interest in studying the coronary blood flow (CBF), therefore we ask for the mesh to be more refined inside the aortic sinus (where CBF comes from) and the coronary roots, while it can be coarser inside the ascending aorta (since the blood flow in this region does not influence CBF). In particular, a constant mesh size was set in each area, being maximum in the ascending aorta and minimum in the coronary roots, and the mesh size was smoothed near the boundary between different areas in order to achieve a continuously varying mesh size. Moreover, a radius dependent mesh size was set in the epicardial coronary arteries by exploiting the computation of the centerlines in this region.
The results of the mesh generation process are depicted in Figure 2a for patient P1. Notice that computational domains for the left ventricles of each patient were generated in [3], as shown in Figure 2b, where both domains are reported for patient P1.

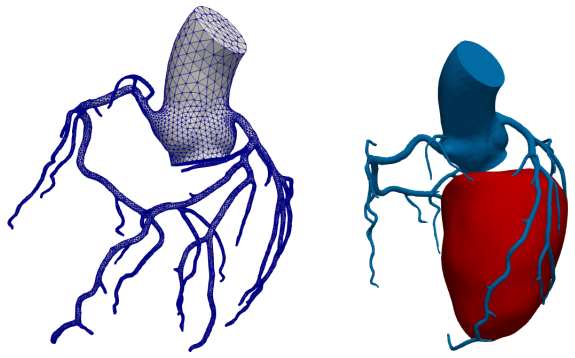

(a) (b)

Figure 2: (a) Patient-specific computational domain of aortic root and epicardial coronary arteries for patient P1. (b) Same domain reported in (a) together with the patient-specific left ventricle generated in [3].

3. Standalone Computational Fluid Dynamics model

As already mentioned in the introduction, we introduced a computational model for hemodynamics inside aortic root and epicardial coronary arteries and applied it to a patient-specific geometry. In particular we considered the domain depicted in Figure 2a, denoted as Ω_{AC}, whose boundary can be divided in: Γ_w, usually denoted as wall and has to be intended as the luminal endothelium; Γ_{in}, aortic inlet cross-section; Γ_{out}, aortic outlet cross-section; Γ^j, coronary outlet cross-sections, where j is the index of each section.
Due to the dimension of the vessels composing the computational domain, 3D NS equations were chosen to regulate blood dynamics in Ω_{AC}. Indeed, in large vessels (down to $\sim 1mm$) it makes sense to model blood as an incompressible, homogeneous, Newtonian fluid [5].
The NS equations of momentum and mass were supplemented with the following boundary conditions:

- homogeneous Dirichlet condition on Γ_w, thus considering the wall as rigid. Such assumption does not hold true in reality, since the aortic root and the coronary arteries are compliant structures able to deform due to the action of blood pressure. Nonetheless, in this first work considering the aortic root, we accepted an approximate solution, ignoring fluid structure interaction;
- Dirichlet condition on Γ_{in}, fixing a flat velocity profile on the aortic inlet section;
- *defective* flow rate condition on Γ_{out}. Due to the chaotic spatial distribution of velocity in the ascending aorta, imposing on the aortic outlet a classical Dirichlet condition, which fixes the spatial velocity profile, would lead to instabilities in the numerical solution. Thus, we opted for a defective condition, only prescribing the flow rate through such boundary;
- Neumann conditions on $\Gamma^j \ \forall j$, thus prescribing the components of the normal Cauchy stress tensor on such boundaries, which, in practice, fixes the pressure values.

In order to guarantee the existence of a solution for a Navier-Stokes problem in classical settings, a number of conditions equal to its spatial dimension has to be prescribed in each point

of the domain boundary [6]. However, on Γ_{out} we are prescribing an average condition, thus the Navier-Stokes problem is not classically well-posed. This is the reason why we have denoted the condition on Γ_{out} as defective. In order to recover a well-posed problem, an augmented reformulation of the NS problem, based on the Lagrange multipliers method [6], was devised. In particular, such formulation selects a particular solution among the infinite solutions of the original problem thanks to implicit Neumann-like boundary conditions, while prescribing the constraint on the flow rate in a weak sense.

Thanks to the Dirichlet condition on Γ_{in} and the defective flow rate condition on Γ_{out}, we managed to prescribe physiological flow rates inside the ascending aorta and the epicardial coronaries arteries, while guaranteeing that the mean flow rate entering the aortic root is about 5 $[L/min]$ and the total flow entering the coronary circulation is 5% of the cardiac output, as expected in physiological conditions. Moreover, we prescribed physiological pressure values on the coronary outlets Γ^j.

For the discretization of the augmented NS problem we followed an approach based on a Finite Element space discretization, using P1/P1 element with a SUPG-PSPG stabilization, and a BDF of order 1 time discretization with semi-implicit treatment of the convective term.

The new contribution of this work was the implementation on the Finite Element library $life^x$ of the numerical methods needed to solve the augmented reformulation of the NS problem based on the Lagrange multipliers method. The implementation was validated on a cylindrical idealized geometry before being exploited to perform numerical hemodynamics simulation inside the patient-specific domain shown in Figure 2a.

In particular, exploiting the implemented Lagrange multipliers method, we were able to effectively prescribe defective flow rate conditions in real geometries, proving the accuracy and robustness of the numerical method.

Moreover, we managed to obtain physiologically consistent numerical results in terms of flow rates, velocity streamlines and pressure values. Indeed:

- the model describes a greater blood flow inside the left coronary tree, as expected;
- the absolute pressure values inside the aortic root vary between $80-120$ $[mmHg]$ during an heartbeat, reaching maximum values during systole and minimum values during late diastole;
- the 3D description allows the model to capture regular velocity streamlines inside the aortic root during systole, while the flow in aorta is accelerating, and secondary flows and recirculating zones during diastole.

Finally, we slightly modified the model setup. Up to this moment we did not consider that the intramural vessels belonging to the left heart are more compressed during systole with respect to the intramural vessels belonging to the right heart, due to higher pressure values in the left side of the heart. In order to account for this feature we prescribed during systole higher pressure values on the coronary outlet sections perfusing the left heart. The numerical results showed that by performing this modification the model is able to capture retrograde flow in the left coronary tree during early systole, whereas in the right coronary tree CBF is always strictly greater than 0, which is a more physiologically consistent result in terms of flow partition. In Figure 3 we report the numerical flow rates in both coronary trees during an heartbeat considering the baseline setup and the modification just presented.

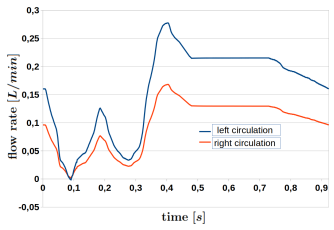

(a)

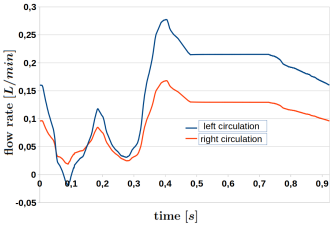

(b)

Figure 3: Flow rates in left and right coronary branches following two strategies: (a) same pressure boundary conditions for left and right heart; (b) account for a pressure correction in left heart during systole.

Such analysis highlights the flexibility of our computational model and its ability to provide very accurate results as long as meaningful boundary conditions are prescribed.

4. Myocardial perfusion model

The aortic hemodynamics model presented in Section 3 was coupled with a 3-compartment Darcy model for the left ventricle in order to numerically simulate cardiac perfusion. In particular, the three Darcy compartments are related to the different length scales of the intramural vessels (arteries, arterioles and capillaries), thus this approach provides a description of blood dynamics inside the capillaries, where oxygen and nutrients exchange happens.
In each compartment $i = 1, 2, 3$ the Darcy model in primal formulation reads:

$$\begin{aligned} -\nabla \cdot (\mathbf{K}_i \nabla p_{M,i}) &= g_i \\ &\quad - \sum_{k=1}^{3} \beta_{i,k}(p_{M,i} - p_{M,k}) \ \text{ in } \Omega_M, \\ (-\mathbf{K}_i \nabla p_{M,i}) \cdot \mathbf{n} &= 0 \qquad\qquad\qquad \text{on } \partial\Omega_M, \end{aligned}$$

where, Ω_M is the myocardial domain, for each $i = 1, 2, 3$, $p_{M,i}$ is the Darcy pore pressure, $\mathbf{K}_i$ is the permeability tensor, g_i is a volumetric source (or sink) term and $\beta_{i,k}$, $k = 1, 2, 3$ $k \neq i$, are the inter-compartment pressure-coupling coefficients. Mass conservation is enforced by compensating the divergence of the Darcy velocity (-$\mathbf{K}_i \nabla p_{M,i}$) in each compartment with a source, or sink, external term (g_i) and mass exchanges between the different compartments ($\beta_{i,k}(p_{M,i} - p_{M,k})$). In particular, only adjacent compartments can exchange mass, so that $\beta_{1,3} = \beta_{3,1} = 0$. Moreover, the intermediate compartment cannot communicate with the external environment, thus $g_2 = 0$. Finally, the third compartment is related to the microvasculature, therefore we need a sink term accounting for the venous return, namely:

$$g_3 = -\gamma(p_{M,3} - p_{veins}),$$

where p_{veins} is the venous pressure and γ a suitable draining coefficient.
The novelty of this study with respect to the model proposed in [2] is the inclusion of the aorta inside the computational domain where 3D Navier-Stokes equations are solved. Thus, we inherited the coupling conditions from [2], whereas we had to define suitable boundary conditions on the aortic inlet and outlet sections. In particular, we considered the same conditions presented in Section 3 for the aortic hemodynamics model, such as a Dirichlet condition on the aortic inlet Γ_{in} and a defective flow rate condition on the aortic outlet Γ_{out} treated with the Lagrange multipliers method.
The two models were coupled by imposing the continuity of mass and momentum, as proposed in [2]. Namely, the NS problem was equipped with suitable Robin-like conditions depending on the pressure field in the first Darcy compartment (most proximal one):

$$\begin{aligned} &\int_{\Gamma^j} \mathbf{u}_{AC} \cdot \mathbf{n} \, d\gamma = \\ &\quad = \alpha^j \Big(\frac{1}{|\Gamma^j|} \int_{\Gamma^j} p_{AC} - \frac{1}{|\Omega_M^j|} \int_{\Omega_M^j} p_{M,1} \Big), \end{aligned}$$

where $\mathbf{u}_{AC}$ and p_{AC} are the NS velocity and pressure field, respectively, Ω_M^j denotes the myocardial perfusion region related to the coronary outlet Γ^j and the parameters α^j were introduce in [2] to regulate the pressure jump between the epicardial coronaries outlet and the first Darcy compartment.
On the other hand, a volumetric source term which depends on the flux through the coronary outlets Γ^j was prescribed in the first Darcy compartment:

$$g_1 = \sum_{j=1}^{N^j} \frac{\chi_{\Omega_M^j}(\mathbf{x})}{|\Omega_M^j|} \int_{\Gamma^j} \mathbf{u}_{AC} \cdot \mathbf{n} \, d\gamma,$$

where $\chi_{\Omega_M^j}(\mathbf{x})$ denotes the characteristic function associated to the perfusion region Ω_M^j.
Therefore, the coupled model depends on a set of physical parameters, such as $\mathbf{K}_i$, $\beta_{i,k}$, γ, p_{veins} and α^j, which have to be correctly estimate in order to obtain accurate perfusion results. For each considered patient (P1, P2, P3, P4) such parameters were estimated in rest conditions in [3] by exploiting the geometrical and fluid dynamics features of a surrogate intramural network generated only using information extracted from the cCTA images. Moreover, in order to compare the numerical results with clinical MBF maps under stress conditions, the model parameters were adjusted in [3] to account for induced hyperemic conditions. In particular two strategies were proposed in [3]: stress *a priori* param-

eter adjustment (only accounting for stress induced conditions) and patient-specific optimization (exploiting the clinical MBF maps to further optimize the parameters).
MBF maps are 3D visualizations of myocardial blood flow which provide a 1 on 1 comparison between computational and clinical data. Indeed, from stress Computed Tomography Perfusion (stress-CTP) images it is possible to extract a 3D visualization of MBF, denoted as $\mathrm{MBF}_{\mathrm{CTP}}$, and the 3D description provided by our model allows us to compute the same visualization from numerical results, denoted as $\mathrm{MBF}_{\mathrm{COMP}}$. In particular $\mathrm{MBF}_{\mathrm{COMP}}$ is defined as the amount of blood reaching the third Darcy compartment, related to capillaries, namely:

$$\mathrm{MBF}_{\mathrm{COMP}} = \beta_{2,3} * (p_{M,2} - p_{M,3}). \qquad (2)$$

In order to numerically solve the coupled model, implicit and explicit iterative splitting strategies for the monolithic problem were proposed in [2], so that the NS and the multi-compartment Darcy sub-problems are solved sequentially. Moreover, we considered a semi-implicit Backward Difference Formulation of order 1 for time discretization, P1/P1 Finite Elements with a SUPG-PSPG stabilization for the NS sub-problem and Q1 Finite Elements for the multi-compartment Darcy sub-problem in primal formulation.
The presented model was applied to patient-specific geometries in order to perform several analysis:

- comparison between explicit and implicit splitting strategies;
- study the impact of a change of the parameters p_{veins} and γ on the pressure fields;
- study the impact of a change of the aortic flow rate on the computation of MBF maps;

The numerical results showed that the explicit version of the iterative splitting strategy is stable in real geometries and provides accurate results during diastole, particularly inside the myocardium, while decreasing the computational cost (1 vs 3.39 iterations). On the other hand, the implicit version should be preferred when one needs to have good accuracy also during systole inside aortic root and epicardial coronaries. Moreover, we can obtain physiological absolute pressure values during diastole both by increasing p_{veins} and by decreasing γ. In particular, an increase of the venous pressure acts as a rigid upward translation of the pressure fields, whereas decreasing the drain coefficient leads to a higher pressure gradient between the last Darcy compartment and the venous system. Thus, an increase of p_{veins} has to be preferred, since it allows us to obtain more accurate absolute pressure value while keeping the pressure inside the capillaries almost constant during an heartbeat, as we expect. Finally, a change of aortic flow rate was found to have a negligible on the computation of $\mathrm{MBF}_{\mathrm{COMP}}$.
Lastly, we assessed the reliability of our computational model in reproducing patient-specific MBF maps under stress conditions. For this validation step we considered only patients P2, P3 and P4, due to a lack of available information for patient P1. In Figure 4 we show a comparison between the computational $\mathrm{MBF}_{\mathrm{COMP}}$ maps and the clinical $\mathrm{MBF}_{\mathrm{CTP}}$ map after the patient-specific parameter optimization for each considered patient.

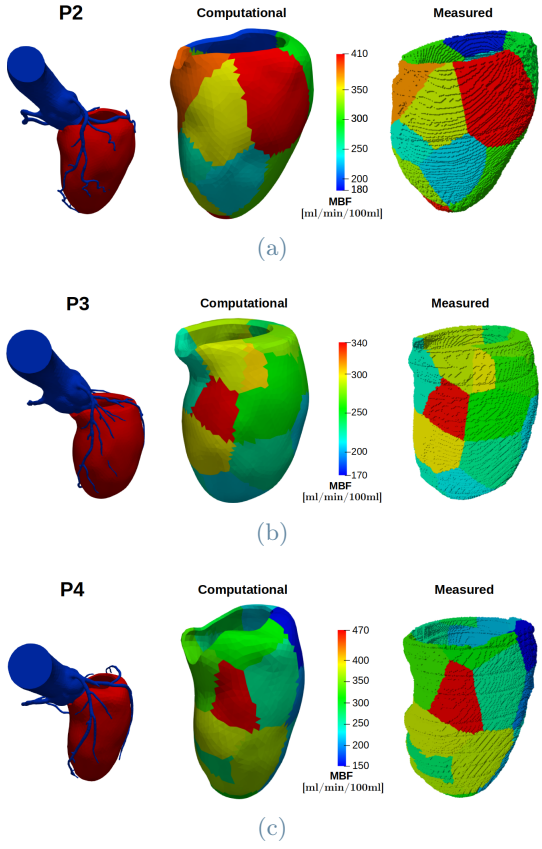

Figure 4: Comparison between $\mathrm{MBF}_{\mathrm{COMP}}$ and $\mathrm{MBF}_{\mathrm{CTP}}$ after the patient-specific parameter optimization for each considered patient.

Figure 4 shows an excellent agreement between

computational and measured maps. Therefore we can conclude that our model is able to provide accurate perfusion results as long as the model parameters are appropriately estimated. In particular, an appropriate estimation of the parameter $\beta_{2,3}$ is crucial to obtain accurate MBF maps, due to the definition of MBF_{COMP} in (2).

5. Conclusions

Leveraging the numerical results obtained both from the standalone CFD model and the myocardial perfusion model we can conclude that the aorta has been successfully included inside the considered modeling framework. Indeed, the standalone CFD model provides physiologically consistent numerical results which can become even more accurate using physically meaningful boundary conditions. Whereas, using the myocardial perfusion model we are able to obtain very accurate perfusion results in terms of MBF maps after a patient-specific optimization of the parameters.

Thanks to the inclusion of the aorta, the mathematical and numerical model for hemodynamics inside aortic root and epicardial coronary arteries can provide meaningful insights on coronary blood flow (CBF). Indeed, the model could be applied to different patient-specific geometries in order to understand the impact of the geometrical features on the blood flow distribution inside the coronary circulation, specially in case of coronary artery diseases. Moreover, 3D blood dynamics simulations could be exploited to quantify the pressure losses in presence of a stenosis and to compute wall shear stresses, which is a key indicator for the development of atherosclerotic plaques. Finally, the inclusion of the aorta allows us to consider aortic valve dynamics in order to evaluate their impact on CBF in future studies.

Moreover, this project represents a first step toward the coupling of myocardial perfusion with ventricular dynamics, such as ventricular electro-mechanics and ventricular ejection. For this reason, this study moves in the direction of a more comprehensive description of the myocardial perfusion process by exploring the model upstream. Additionally, also a downstream extension of the model can be considered in future studies in order to achieve a circular coupling of myocardial perfusion: going from electro-mechanics in the ventricle, to ventricular ejection, to myocardial perfusion, to oxygen exchange in the cardiac capillaries and back to electro-mechanics. Such circular coupled model could be exploited in order to study the impact of perfusion defects on oxygen supply and subsequent propagation of the electrical signal and contraction of the heart muscle, which regulate the cardiac function.

References

[1] J. A. E. Spaan et al. Visualisation of intramural coronary vasculature by an imaging cryomicrotome suggests compartmentalisation of myocardial perfusion areas. *Medical and Biological Engineering and Computing*, 43(4):431–435, 2005.

[2] S. Di Gregorio et al. A computational model applied to myocardial perfusion in the human heart: From large coronaries to microvasculature. *Journal of Computational Physics*, 424:109836, 2021.

[3] S. Di Gregorio and C. Vergara et al. Prediction of myocardial blood flow under stress conditions by means of a computational model. *European Journal of Nuclear Medicine and Molecular Imaging*, 49(6):1894–1905, 2022.

[4] M. Fedele and A. Quarteroni. Polygonal surface processing and mesh generation tools for the numerical simulation of the cardiac function. *International Journal for Numerical Methods in Biomedical Engineering*, 37(4):e3435, 2021.

[5] A. Quarteroni et al. *Mathematical Modelling of the Human Cardiovascular System: Data, Numerical Approximation, Clinical Applications*. Cambridge University Press, 2019.

[6] L. Formaggia et al. Numerical treatment of defective boundary conditions for the Navier–Stokes equations. *SIAM Journal on Numerical Analysis*, 40(1):376–401, 2002.